

## FORCES ON THE BODY DURING ELITE COMPETITIVE PLATFORM DIVING

Simon M. HARRISON<sup>1\*</sup>, Raymond C. Z. COHEN<sup>1</sup>, Paul W. CLEARY<sup>1</sup>, Sian BARRIS<sup>2</sup>, Graeme ROSE<sup>3</sup>

<sup>1</sup> CSIRO Mathematics, Informatics and Statistics, Clayton, Victoria 3168, AUSTRALIA

<sup>2</sup> Skill Acquisition, Biomechanics and Performance Analysis, Australian Institute of Sport, Brisbane, Australia

<sup>3</sup> Diving Australia, Brisbane, Australia

\*Corresponding author, E-mail address: Simon.Harrison@csiro.au

### ABSTRACT

Impact with the water during a 10 m platform dive imparts large forces onto the diving athlete. Wrist and back injuries are common and are thought to be related to cumulative damage from many overload events, rather than one acute high loading event. Experimental measures of forces on the body are impractical and instead computational simulation is appropriate to estimate this loading. A coupled Biomechanical-Smoothed Particle Hydrodynamics (BSPH) model is applied to a reverse pike dive performed by an elite athlete. The skin surface is represented by a mesh that deforms in response to measured skeleton kinematics. Calculations of the impact forces and the transmission of torque through the skeleton are made. The sensitivity of the results of the model to water entry angle is explored. The simulation framework presented shows promise as a tool for coaches to evaluate the performance and safety of diving technique.

### INTRODUCTION

Most competitive platform diving injuries occur during water entry (Rubin, 1999). Injuries sustained during diving can either result from catastrophic overloading of joints during a poorly executed dive or, more commonly, from repetitive loading at lower levels of force, such as during a successful dive. An understanding of how these injuries occur will require detailed information about the mechanical loading of the joints during impact with the water. Biomechanical analysis of the loading on the body during water impact is sparse (Rubin, 1999; Sanders and Burnett, 2003), because direct experimental measurement of loading on the joints and bones is not possible.

Computational biomechanical modelling of sporting activities has previously elucidated the causation of injury through calculation of the mechanical loading of joints, bones, muscles and connective tissue, e.g., during a fall, Keyak et al., 1997; and during running, Schache et al. 2010. Computational simulation provides measures of experimentally immeasurable quantities such as net joint torque; joint power; joint, muscle and tendon forces; and articular stresses. High levels of joint torque are a useful (and easily calculated) indicator of large internal forces, and are highly correlated to injury risk in many activities (e.g. Hewett et al., 2005).

Simulations of the flight phase of platform diving have recently been used to understand and evaluate flight phase performance (e.g. Koschorreck and Mombaur, 2012), but no models of dynamic fluid interactions with the body during platform diving presently exist.

Computational simulation of platform diving presents significant modelling challenges. The athlete is travelling at very high speed at the time of impact with the water and the pose of the athlete's body changing significantly and rapidly during interaction with the water. The free surface of the water also experiences large displacements and fragmentation/splashing during entry by the athlete's body. Smoothed Particle Hydrodynamics is a Lagrangian particle method that is well suited to transient problems with complex free surface behaviour, and moving and deforming boundaries of complicated shape. Recent work in swimming (Cohen and Cleary, 2010; Cohen et al., 2011; Cohen et al., 2012) has shown the viability and usefulness of this method for water-based sports.

A computational modelling framework for competitive platform diving using a coupled Biomechanical-SPH model is proposed. The purpose of this study is to explore the following issues:

1. What are the magnitudes of forces imparted onto different body segments during water entry for a reverse pike dive?
2. What is the torque generated in the wrists and back during water entry?
3. How does this torque loading change when the angle of entry is rotated by 5 and 10 degrees?

To answer these questions, the kinematic motion of an Australian Olympic athlete was digitised during a reverse pike dive. This motion was used to deform a boundary representation of her body during a computational simulation of the dive. Simulations using 5 and 10 degree variants to the angle of entry were performed. Whole body motion, fluid forces on the body joint segments and net torques about the joints were calculated.

### COMPUTATIONAL MODEL

#### Smoothed Particle Hydrodynamics

Smoothed Particle Hydrodynamics (SPH) is a mesh-free Lagrangian particle method for solving partial differential equations. Fluid dynamics applications of the method are detailed in Monaghan (1994), Monaghan (2005) and Cleary et al. (2007). Volumes of fluid are represented by a moving set of particles, over which the Navier Stokes equations can be reduced to the following ordinary differential equations:

$$\frac{d\rho_a}{dt} = \sum_b m_b \mathbf{v}_{ab} \cdot \nabla_a W_{ab} \quad (1)$$

where  $\rho_a$  is the density of particle  $a$ ,  $t$  is time,  $m_b$  is the mass of particle  $b$  and  $\mathbf{v}_{ab} = \mathbf{v}_a - \mathbf{v}_b$ , where  $\mathbf{v}_a$  and  $\mathbf{v}_b$  are the velocities of particles  $a$  and  $b$ .  $W$  is a cubic-spline interpolation kernel function that is evaluated for the distance between particles  $a$  and  $b$ .

$$\frac{d\mathbf{v}_a}{dt} = -\sum_b m_b \left[ \left( \frac{P_b}{\rho_a^2} + \frac{P_a}{\rho_b^2} \right) - \frac{\xi}{\rho_a \rho_b} \frac{4\mu_a \mu_b}{(\mu_a + \mu_b)} \frac{\mathbf{v}_{ab} \cdot \mathbf{r}_{ab}}{\mathbf{r}_{ab}^2 + \eta^2} \right] + \mathbf{g} \quad (2)$$

where  $P_a$  and  $\mu_a$  are the local pressure and dynamic viscosity for particle  $a$ ,  $\eta$  is a small number to mitigate singularities when the denominator is small,  $\xi$  is a normalisation constant for the kernel function and  $\mathbf{g}$  is the gravitational acceleration.

A quasi-compressible formulation of the SPH method is employed. The equation of state for such a weakly compressible fluid relates the fluid pressure,  $P$  to the particle density,  $\rho$ :

$$P = \frac{c^2 \rho_0}{\gamma} \left[ \left( \frac{\rho}{\rho_0} \right)^\gamma - 1 \right] \quad (3)$$

where  $c$  is sound speed and the reference density is given by  $\rho_0$ .  $\gamma$  is a material constant, which is equal to 7 for fluids with properties similar to water. A mach number of approximately 0.1 is used to reduce density variations from compressibility effects to the order of 1%.

Nodes of boundary objects are represented as boundary SPH particles, which are repositioned at every time step as a result of any rigid body motion and/or deformation of the boundary. The boundary of the athlete's body (described below) was allowed to move dynamically in all six degrees of freedom during simulation. The moments of inertia of the athlete were calculated from the athlete's mass and volume, assuming a homogeneous distribution of density.

#### SPH model of the pool

A stagnant pool of water 5 m deep, 2 m wide and 4 m long was modelled. The water was represented by 13.2 M SPH particles with separations of 15 mm. Periodic boundary conditions were used in both horizontal directions.

#### Biomechanical model of the diving athlete

##### Surface mesh of the athlete's body

The athlete's body was represented in the computational model by a deforming surface mesh. The mesh of 51,000 nodes, spaced at an average separation of 10 mm, was constructed from 3D laser scans (VITUS Smart XXL machine; Human Solutions GmbH, Kaiserslautern, Germany) of one Australian Olympic athlete. The mesh was rigged to a virtual skeleton using the dual quaternion method (Kavan et al., 2008). This rigged mesh was deformed by manipulation of the virtual skeleton to produce specific poses that matched video footage of platform dives by the laser scanned athlete.

##### Kinematics digitisation

Footage from four temporally-synchronised, fixed position cameras was supplied for a reverse pike dive. The rigged surface mesh of the athlete's body was positioned using Autodesk Maya software (Autodesk Inc., San Rafael, CA, USA), to simultaneously match top, side (one above the water and one below) and rear views of each dive, at each frame of the video footage. Two of the views are shown in Figure 1. The athlete kinematics were used to deform the skin mesh at each time in the simulation.

##### Kinetic analysis

Linear forces and torques exerted onto the diver boundary mesh predicted by interactions of boundary particles with fluid particles were calculated for the whole body and for

individual joints. The linear force,  $\mathbf{f}_{\text{obj}}$ , acting on an object of interest was calculated by summing the individual boundary forces,  $\mathbf{f}_i$ , that act on all parts of that body.

$$\mathbf{f}_{\text{obj}} = \sum_{i=1}^N \mathbf{f}_i \quad (4)$$

Similarly the net torque,  $\mathbf{T}_{\text{obj}}$ , about an object was calculated as the vector sum of the cross product of each boundary force,  $\mathbf{f}_i$ , with the position vector of the boundary particle,  $\mathbf{u}_i$ , in the reference frame of the object (which is the joint centre for joints):

$$\mathbf{T}_{\text{obj}} = \sum_{i=1}^N \mathbf{u}_i \times \mathbf{f}_i \quad (5)$$

#### Sensitivity analysis

To understand the sensitivity of predictions to model inputs, the following cases were simulated:

- Case 1. As digitised
- Case 2. Sagittal plane rotation (pitch angle) increased by 5 degrees prior to water impact
- Case 3. Sagittal plane rotation (pitch angle) increased by 10 degrees prior to water impact

The sensitivities of body forces and distal arm joints to these variations were calculated. Cases 2 and 3 represent poorly executed dives with over-rotation.

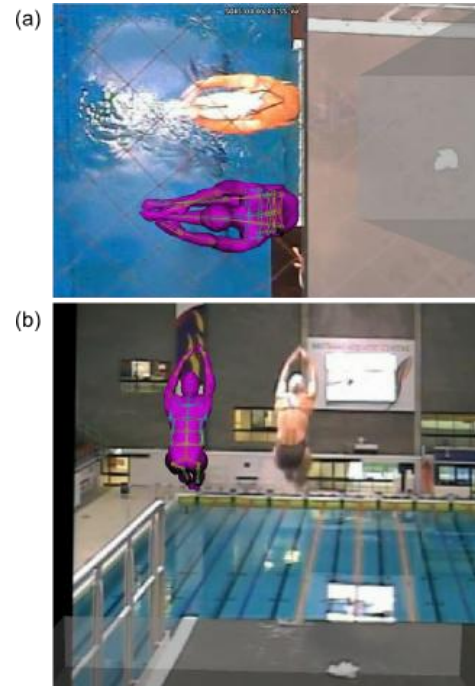


**Figure 1:** Digitisation of the athlete for the reverse pike dive. Top (a) and rear (b) viewing angles are shown.

#### RESULTS AND DISCUSSION

The simulated motion of the athlete during the reverse pike is shown in Figure 2. The reverse pike involves a forwards leap (0.0 s to 1.0 s), followed by a backwards rotation whilst the hands touch the legs near the feet (until 1.07 s), and then a straightening of the body as the half backwards somersault is completed (1.33 s onwards). The body then enters the water (at 2.36 s) in an approximately vertical orientation with the hands held flat as they impact the water. After water entry the body continues to translate and rotate in the same direction, albeit at a slower pace due to slowing effect of the water drag.

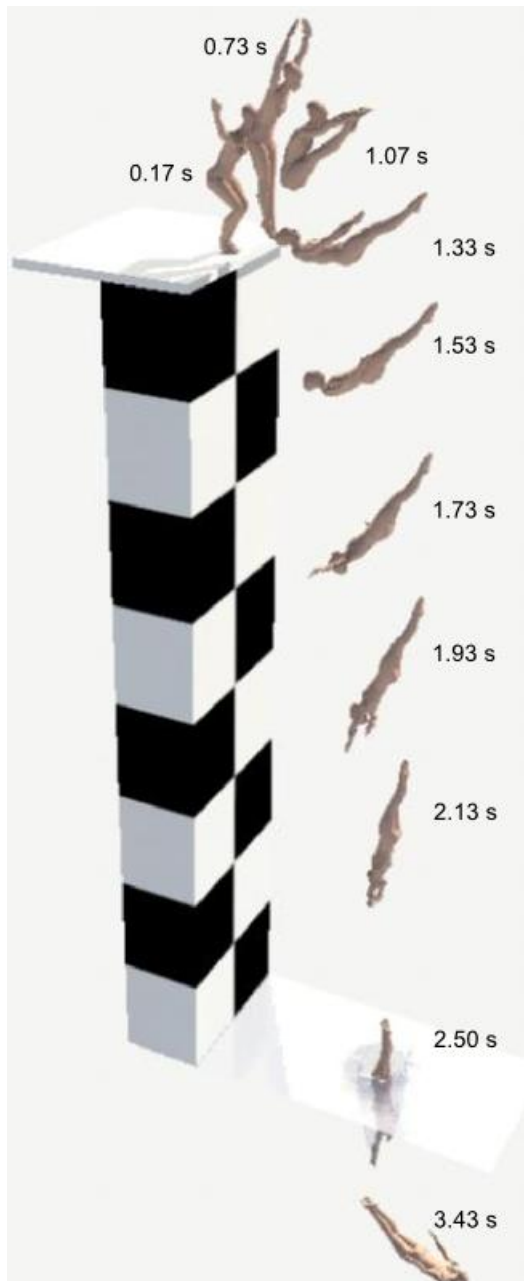


**Figure 2:** Motion of the athlete for the digitised reverse pike dive.

Figure 3 shows the magnitude of force exerted on each major body segment and the total magnitude of force exerted on the body. Peaks of force occur as each body segment first makes contact with the water. The hand forces are the largest and their peak occurs almost immediately after water impact. The hand forces then decline in magnitude until 2.76 s, when a small peak occurs as the arms sweep from a position above the head to a position beside the torso. Total body forces peak once all body segments have made contact with the water (2.57 s) representing the period of maximum drag by the fluid on the diver. This peak coincides with high levels of force in the forearms, shoulders and head, lower back and legs. Forces decline once complete immersion of the body has occurred (at 2.69 s), but increase again as skin drag between the water and the completely immersed body of the diver (2.70 s onwards) is at a maximum.

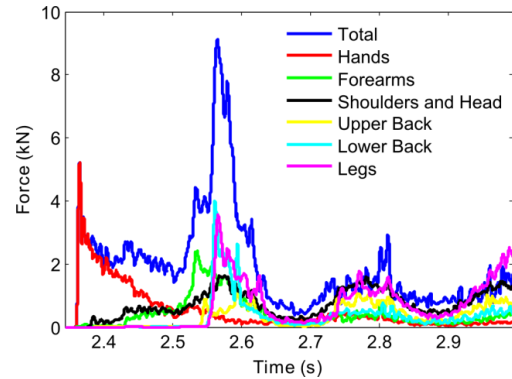


**Figure 3:** Magnitudes of fluid force on the segments of the body after water entry at  $t = 2.36$  s.

### Sensitivity analysis

The motion of the athlete and the athlete-water interactions change when the entry pitch angle is altered. Figure 4 shows the pitch angle, the vertical speed and the vertical position of the diver from the time of water entry. During the as digitised dive (Case 1) the body does not pitch significantly before 2.53 s (Figure 4a). After this the pitch angle decreases quickly over 200 ms and then gradually decreases further. However, as the entry pitch angle is increased (Cases 2 and 3 respectively), the body pitches further earlier and to a larger degree. The vertical speed decreases more quickly with increasing initial pitch angle (Figure 4b). As a result the dive trajectory becomes progressively shallower (Figure 4c).

The athlete's position, the fluid free surface, and the 3D vortex structures are shown in Figure 5 for all three cases. For Case 1 the body is approximately vertical until almost fully immersed (2.53 s). The area of the diver projected into the horizontal plane (which is orthogonal to the motion of the diver and controls the drag) is minimal. The fluid free surface near the body has been displaced downwards into a cavity (see Brown et al., 1984; in approximate forwards-rear symmetry about the body). The presence of the cavity delays interactions between the water and the body below the shoulders, even though the entire body is below the initial water level. At 2.67 s all the body below the lower legs is fully immersed and at 2.80 s the body becomes completely immersed in the water. Vortex structures are progressively shed from the hands, arms, torso and legs as the energy is transferred to the fluid and the body is decelerated.

As the initial pitch rotation increases the behaviour of the fluid and the athlete changes significantly. For Case 2 the body pitch increases strongly and quickly and the water cavity left behind by the body is larger in the forwards-rear direction (see Figure 5, at  $t = 2.53$  s). The volume of water displaced is larger than for Case 1. The front side of the body from hands to shins have made contact with the water, changing the timing of fluid loading on the body. Due to the larger forwards-rear size of the induced water cavity, the vortex structures occupy a larger volume and the amount of splash is larger, extending both higher and wider. For Case 3, the cavity is even larger in the forwards-rear direction at 2.53 s. The entire body makes contact with the water meaning that the distribution and magnitudes of force are changed. The volume of displaced water and the size of the splash are further increased. These results suggest a direct relationship between angle of entry and the size of the splash and the magnitude and distribution of fluid forces on the body.

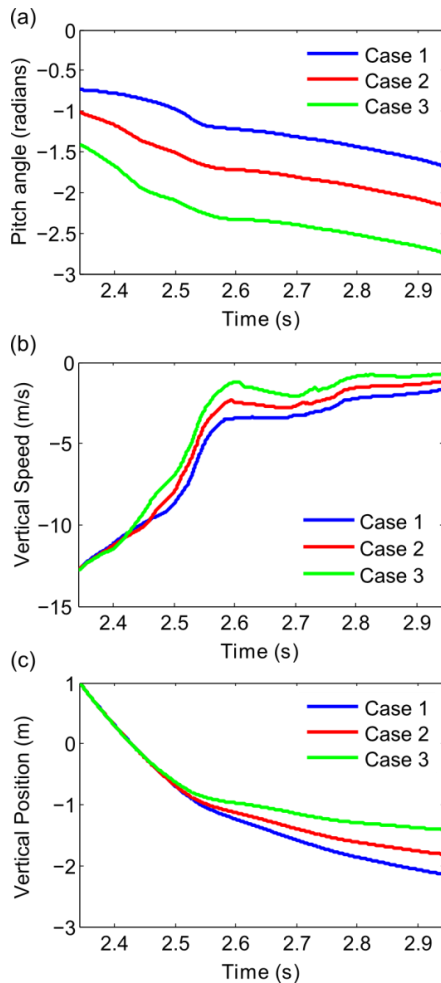


**Figure 4:** Pitch angle, vertical speed and vertical position of the centre of mass of the diver from the time of water entry (at  $t = 2.36$  s), for the three entry pitch angles.

The differences in interaction between the athlete's body and the water for the three cases can be related to the differences in kinematics. As the entry pitch angle increases the projected area of the athlete into the plane of the water surface increases markedly. A larger projected area equates to larger drag forces from the water. These larger drag forces decelerate the athlete in a shorter amount of time.

The fluid force on the hands and torso are compared in Figure 6 for the three entry pitch angles. The fluid forces on the hands are very similar for all three cases, with only a small decrease with increasing angle. This is because the hands interact with the same undisturbed fluid at the same vertical speed. However, the first peak of force on the torso occurs earlier with increased pitch angle because the body rotates quicker and impacts the water earlier (see Figs 4 and 5). The force behaviour becomes similar again for all three cases after the torso is submerged (at 2.53 s). These earlier peaks of force on the torso in Cases 2 and 3 are additional loads on the body, which could add to injury risk.

Even though the extent of the variations in the fluid forces is not large, there is a strong dependence of peak joint torque on entry pitch angle. The net joint torques on the wrists are shown in Figure 7. They display two distinct peaks, one just after water impact and the other corresponding to when the arms move from above the head to the sides. In all three cases the magnitudes of joint

torque are very large and near to the maximal limits of human abilities (Fukunaga et al., 2001). The net torques, particularly their peaks, increase with increasing pitch angle. In all cases, the net torque about the left wrist joint is approximately equal to that about the right wrist (which is not unreasonable since the dive is symmetric from left to right of the diver).

The joint torques are larger for the back than for the wrists and also dependent strongly on entry pitch angle (shown in Figure 8). They peak when the front of the torso makes contact with the fluid. This occurs earlier as the pitch angle increases. The torque in the lower back are larger than for the upper back, suggesting higher muscle and ligament forces and a larger risk of injury.

Whilst the peak fluid forces on the hands and torso did not increase significantly with increasing pitch angle, the wrist and back joint torques did increase strongly. As pitch angle increases, the body is less optimally posed to absorb the impact force from the water. The larger joint torques during Case 2 and Case 3 indicate that higher loading on the ligaments of the joints will occur and that larger muscle forces will be needed to stabilise the arm joints and the lower back during impact with the water. These larger forces are more likely to cause injuries.

The importance of correct joint orientation in relation to the direction of fluid loading is also indicated by the differing timing of peaks of force and joint torque. For instance, whilst fluid forces on the hand peak sharply within the first 100 ms, the joint torques at the wrists are large over the first 600 ms. These results suggest that analysis of fluid forces on limb segments alone is not sufficient for determining the timing and locations of possible injurious loading during diving.

As high joint torques are an indicator of injury likelihood, our simulation results suggest that

1. the likelihood of musculoskeletal injury in the joints of the arm and the back is high, especially during the first 600 ms of water impact and when the arms are used to slow the body; and
2. the likelihood of musculoskeletal injury in the wrists and back increases strongly when the pitch angle increases away from a vertical entry.

It is worth noting that the joint torques may vary significantly when the form of the dive is altered, such as when somersaults and/or twists are added or when a rip entry is used (Brown et al., 1984). This will be the subject of future studies.

## CONCLUSION

A coupled Biomechanical-SPH model of platform diving was developed. Using both digitised motion and a 3D laser scan of an Olympic athlete, a dynamic simulation, including water and diver-water interactions, of a reverse pike dive was performed. The effect of entry pitch angle was also explored. Dynamic interaction between the diver and the water and joint torques has not previously been predicted. The novel simulation framework allows the prediction of forces imparted onto the body and the resulting torques that are generated at key joints. This broadens the options for evaluation and optimisation of the performance of an athlete and the water behaviour resulting from the dive.

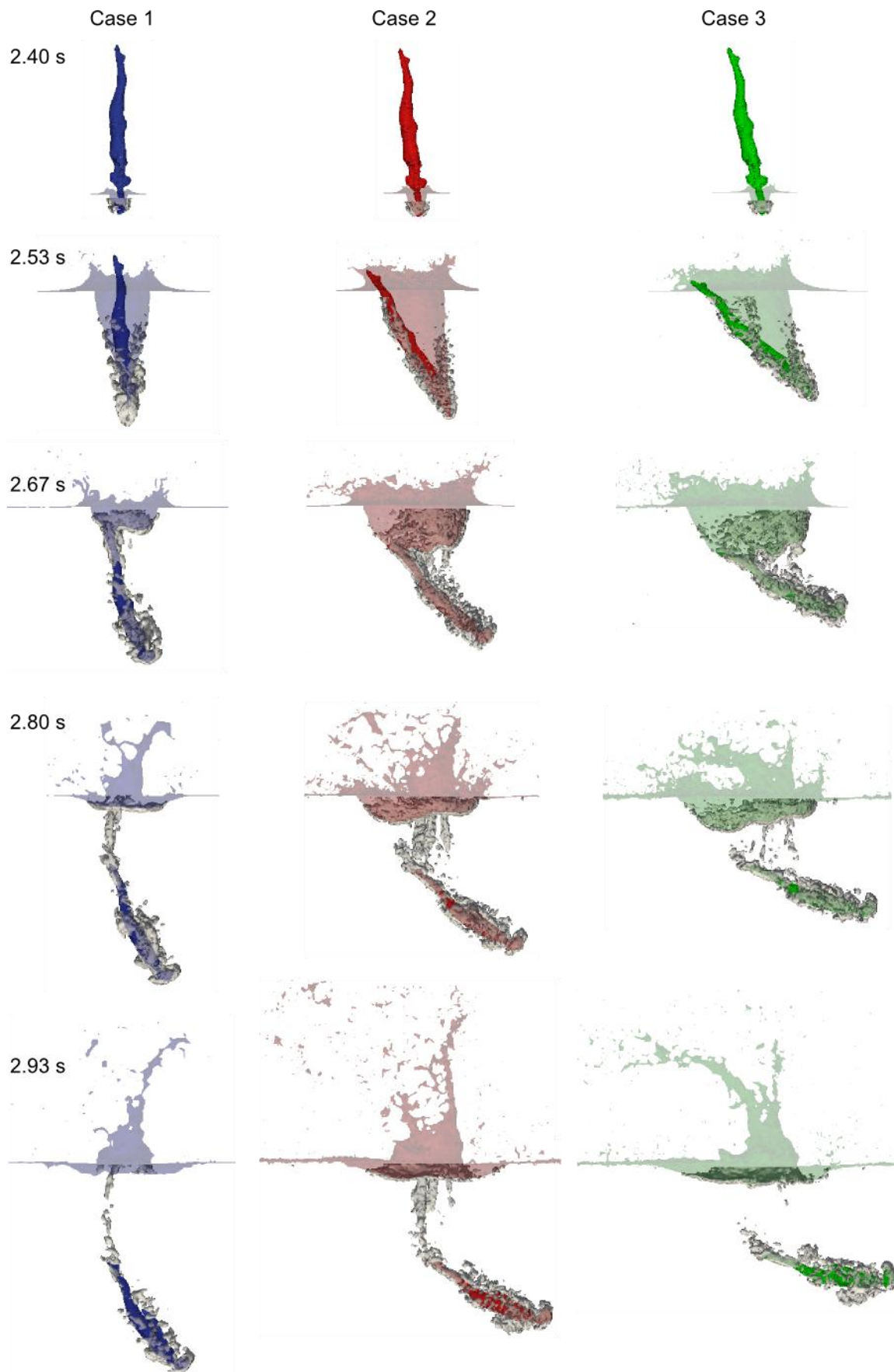


**Figure 5:** Visual comparison of the motion of the diver, the fluid free surface and 3D vortex structures for the three simulation cases ( $0^\circ$ ,  $5^\circ$  and  $10^\circ$  offset entry pitch angle). The rows show the situation at five times from initial water impact onwards.

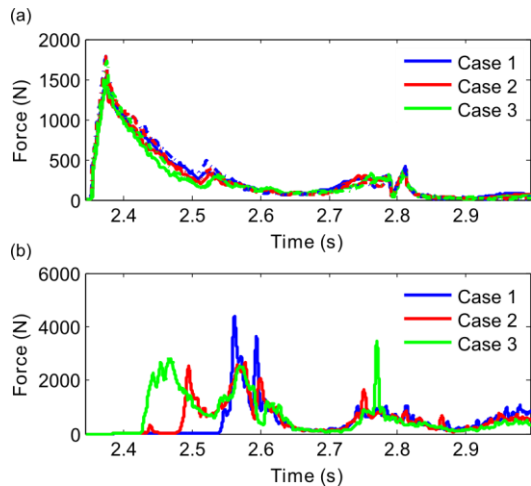


**Figure 6:** Magnitude of net force on (a) the hands and (b) the torso after water entry at  $t = 2.36$  s for the three entry pitch angles.

Simulation results indicated that the body is decelerated over a small time period, resulting in large forces being imparted to the body by the water. Joint torques were large for all simulation cases, suggesting the presence of large muscle, ligament and joint forces in the wrists and lower back. These large loads are likely to be correlated to the known high risk of injuries to the wrists and lower back. Larger joint torques occurred in the wrists and the back as entry pitch angle was increased. As fluid forces on the hands and torso did not show the same dependence on pitch angle, the orientation and pose of the body must be the critical determinants of torque magnitude. Future work will investigate these relationships for more complicated dives and entries, and will involve the calculation of muscle and joint forces.

## REFERENCES

BROWN, J.G., ABRAHAM, L.D., BERTIN J.J., (1984), "Descriptive analysis of the rip entry in competitive diving", *Research Quarterly for Exercise and Sport*, 35(2), pp. 93-102

CLEARY PW, PRAKASH M, HA J, STOKES N, SCOTT C (2007) "Smooth particle hydrodynamics: status and future potential", *Prog Comput Fluid Dy* 7 70-90

COHEN, R.C.Z., CLEARY, P.W., (2010), "Computational studies of the locomotion of dolphins and sharks using Smoothed Particle Hydrodynamics", in: *Proceedings of the 6th World Congress of Biomechanics (WCB 2010)*, IFMBE Proceedings. Springer, Singapore Suntec Convention Centre, pp. 22-25.

COHEN, R.C.Z., CLEARY, P.W., MASON, B.R., (2011), "Simulations of dolphin kick swimming using smoothed particle hydrodynamics". *Hum Movement Sci*, 31(3), 604-619.

COHEN, R.C.Z., CLEARY, P.W., MASON, B., PEASE, D.L., "Relating kinematics to performance in freestyle swimming using Smoothed Particle Hydrodynamics". *Submitted to Hum Movement Sci*

FUKUNAGA, T., MIYATANI, M., TACHI, M., KOUZAKI, M., KAWAKAMI, Y. AND KANEHISA, H. (2001), "Muscle volume is a major determinant of joint torque in humans" *Acta Physiologica Scandinavica*, 172, 249-255.

HEWETT, T. E., MYER, G. D., FORD, K. R., HEIDT, R. S., COLOSIMO, A. J., MCLEAN, S. G., VAN DEN BOGERT, A. J., PATERNO, M. V. AND SUCCOP, P.

(2005), "Biomechanical Measures of Neuromuscular Control and Valgus Loading of the Knee Predict Anterior Cruciate Ligament Injury Risk in Female Athletes.", *The American Journal of Sports Medicine*, 33, 492-501.

KAVAN, L., COLLINS, S., ZARA, J., O'SULLIVAN, C., (2008), "Geometric Skinning with Approximate Dual Quaternion Blending" *ACM Transaction on Graphics*, 27(4), Article 105, pp. 1-23.

KEYAK, J.H., ROSSI, S.A., JONES, K.A. and SKINNER, H.B. (1997), "Prediction of femoral fracture load using automated finite element modeling" *J Biomech*, 31, 125-133.

KOSCHORRECK, J. AND MOMBAUR, K. (2012), "Modeling and optimal control of human platform diving with somersaults and twists", *Optimization and Engineering*, 13, 29-56.

MONAGHAN, J.J. (1994), "Simulating free surface flows with SPH", *J Comput Phys* 110(2), 399-406

MONAGHAN, J.J. (2005) "Smoothed particle hydrodynamics", *Rep Prog Phys* 68, 1703-1759

RUBIN, B.D. (1999), "The basics of competitive diving and its injuries" *Clin Sports Med*, 18, 293-303.

SANDERS, R. and BURNETT, A. (2003). Diving. *Sports Biomech*, 2, 251-264.

SCHACHE, A.G., KIM, H.-J., MORGAN, D.L. and PANDY, M.G. (2010), "Hamstring muscle forces prior to and immediately following an acute sprinting-related muscle strain injury" *Gait Posture*, 32, 136-140.

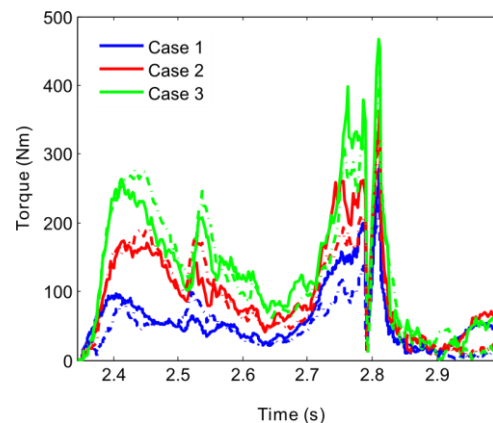


**Figure 7:** Magnitude of net torque about the right wrist joint (solid lines) and the left wrist joint (dashed lines) after water entry at  $t = 2.36$  s for the three entry pitch angles.

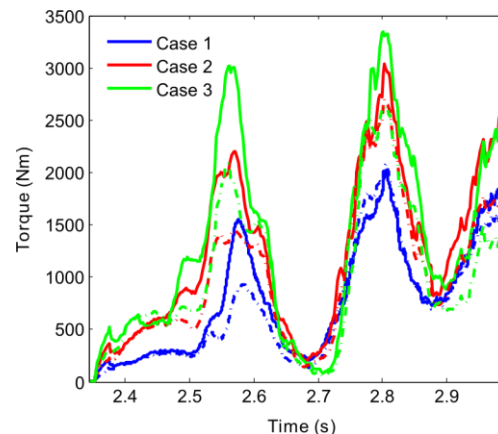


**Figure 8:** Magnitudes of net torque about the upper back (dashed lines) and lower back (solid lines) after water entry at  $t = 2.36$  s for the three entry pitch angles.